Reductive Elimination and Isomerization of Organogold Complexes. Theoretical Studies of Trialkylgold Species as Reactive Intermediates

Sanshiro Komiya,[1a] Thomas A. Albright,[1b] Roald Hoffmann,*[1b] and Jay K. Kochi*[1a]

Contribution from the Departments of Chemistry, Indiana University, Bloomington, Indiana 47401, and Cornell University, Ithaca, New York 14850.
Received April 15, 1976

Abstract: Trialkyl(phosphine)gold complexes R_3AuL are involved in facile reductive elimination as well as cis-trans isomerization. Deuterium labeling studies show that elimination, but not isomerization, proceeds via two competing pathways. The intermolecular route predominates in nonpolar solvents such as decalin and benzene, whereas dimethyl sulfoxide (Me_2SO) and dimethylformamide promote the intramolecular reactions. Kinetic studies support trialkylgold species, R_3Au, formed by the rate-limiting dissociation of phosphine, as the common intermediate in both cis-trans isomerization and reductive elimination. Capture of R_3Au by Me_2SO prevents its association with other alkylgold species to promote further intermolecular reactions, and only intramolecular processes leading to isomerization and reductive elimination are observed in this solvent. We calculate from the kinetic results that the coordinatively unsaturated intermediate $Et(CH_3)_2Au$ undergoes isomerization between T-shaped configuration 100 times faster than reductive elimination. Molecular orbital calculations indicate that the potential energy surface for $(CH_3)_3Au$ is determined by the orbital degeneracy of the symmetrical C_{3h} geometry, and favor distortion to T- and Y-shaped configurations of lower energies. The former represent minima, and the Y-shaped configurations are saddle points for the cis-trans isomerization of the T's and serve as exit channels through which reductive elimination proceeds. Deuterium labeling studies show that methyl-methyl coupling between dimethylcuprate(I) and methyl iodide or trifluoromethanesulfonate occurs without scrambling. *If* trimethylcopper species are formed as intermediates similar to the gold analogue, then the reductive elimination of methyl groups must also proceed via T-shaped configurations.

Alkylgold complexes, among organic derivatives of transition metals, serve as excellent models for catalytic studies since the thermal decomposition of analogues such as I result in the coupling of alkyl groups (eq 1) rather than disproportionation (eq 2).[2] Carbon-carbon bond formation in this manner, when

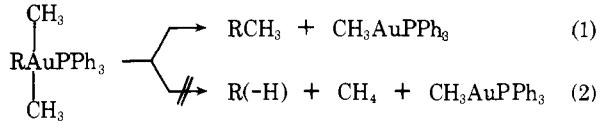

$$RCH_3 + CH_3AuPPh_3 \quad (1)$$

$$R(-H) + CH_4 + CH_3AuPPh_3 \quad (2)$$

I

it is accompanied by an oxidative addition process in a subsequent step, provides an attractive mechanistic pathway by which various metal complexes catalyze the coupling of Grignard and organolithium reagents (Rm) with alkyl halides in eq 3.[3]

$$Rm + R'X \xrightarrow{[M]} RR' + mX \quad (3)$$

The mechanism of decomposition of alkylmetal species like I is thus central to the understanding of such a catalytic cycle.

Three separate reactions can be observed independently when a variety of alkyldimethyl(triphenylphosphine)gold complexes are heated,[2] viz., (i) alkyl rearrangement, (ii) cis-trans isomerization, and (iii) reductive elimination as represented below where L = PPh_3. Retardation by added tri-

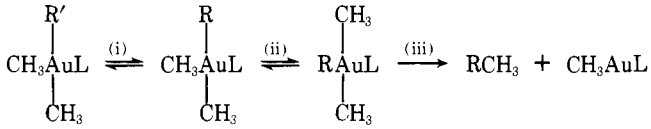

$$\xrightarrow{(i)} \quad \xrightarrow{(ii)} \quad \xrightarrow{(iii)} \quad RCH_3 + CH_3AuL$$

phenylphosphine together with ^{31}P NMR results, led to the earlier conclusion that a three-coordinate trialkylgold species II was an intermediate in the reductive elimination of I. On the other hand, since the cis-trans isomerization of I is relatively unaffected by the presence of excess triphenylphosphine, it suggested that the isomerization occurs via an independent

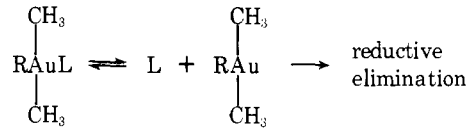

reductive elimination

I II

unimolecular process involving the undissociated trialkyl(triphenylphosphine)gold complex itself. The latter leaves open the interrelationship between cis-trans isomerization and reductive elimination of I, particularly with regard to the role of the important three-coordinate intermediate II in the isomerization. Furthermore, the structure and reactivity of the coordinatively unsaturated species II, as well as the mechanism by which it undergoes reductive elimination, remain largely unexplored.

In this study, both intermolecular and intramolecular processes in the cis-trans isomerization and reductive elimination of trialkyl(phosphine)gold complexes have been delineated by the use of deuterium labeling and kinetic studies. The stereochemistry of reductive elimination and cis-trans isomerization, both proceeding via a three-coordinate trialkylgold intermediate, are related to a theoretical model using molecular orbital calculations to describe T- and Y-shaped configurations along the potential energy surface leading to cis-trans isomerization and reductive elimination. These results are finally related to the facile copper(I)-catalyzed coupling described in eq 3.

Results and Discussion

Reductive Elimination of Trimethyl(triphenylphosphine)gold. Trimethyl(triphenylphosphine)gold is a square planar d^8 complex, judging from its diamagnetism and NMR spectrum.[4] In the absence of phosphine ligand, trimethylgold is extremely unstable and has not yet been isolated.[5] Thermal decomposition of $(CH_3)_3AuPPh_3$ affords ethane and CH_3AuPPh_3, which itself undergoes further decomposition to ethane and a gold mirror according to eq 4 and 5, respectively.[2,6]

$$(CH_3)_3AuPPh_3 \rightarrow CH_3CH_3 + CH_3AuPPh_3 \quad (4)$$

$$CH_3AuPPh_3 \rightarrow \tfrac{1}{2}CH_3CH_3 + Au^0 + PPh_3 \quad (5)$$

Table I. Thermal Decomposition of $Me_3Au(PPh_3)$ and $(CD_3)_3Au(PPh_3)$[a]

Time (min)	$(CH_3)_3Au(PPh_3)$ (mg)	$(CD_3)_3Au(PPh_3)$ (mg)	Solvent	Concn (mM)	Evolved gas (%) C_2D_6	CH_3CD_3	C_2H_6
15	6.5	6.5	$C_{10}H_{18}$	0.5	32	24	45
2	12.5	12.5	$C_{10}H_{18}$	2.5	40	25	35
10	16.0	16.0	$C_{10}H_{18}$	10.6	34	29	37
2	36.8	36.8	$C_{10}H_{18}$	146	24	45	31
10	36.9	36.9	PhCl	146	36	36	28
5	12.5	12.5	n-Bu_2O	2.5	40	29	31
10	12.5	12.5	THF	2.5	34	22	44
10	12.5	12.5	DMF	2.5	50	4	46
10	12.5	12.5	Me_2SO	2.5	51	1	48
10	46.6	46.6	Me_2SO	92.5	47	5	48
5	63.2	63.2	C_6H_6	179	37	27	36
5	*b*	*b*	Me_2SO	—	48	0	52

[a] Reaction time is 5–15 min at 80 °C, corresponding to less than 20% decomposition. [b] Sample obtained from the partially decomposed solution in benzene listed above, reisolated and dissolved in Me_2SO.

In the presence of triphenylphosphine, the decomposition can be largely interrupted after the first stage.

We examined first the participation of intermolecular and intramolecular processes in reductive elimination by deuterium labeling in two systems, (a) mixtures of $(CH_3)_3AuPPh_3$–$(CD_3)_3AuPPh_3$ and (b) *cis*- or *trans*-$CD_3(CH_3)_2AuPPh_3$, respectively.

A. Intermolecular Studies of the Reductive Elimination of Mixtures of $(CH_3)_3AuPPh_3$ and $(CD_3)_3AuPPh_3$. The thermal decomposition of tris(trideuteriomethyl)(triphenylphosphine)gold in decalin solution afforded only perdeuterioethane.

$$(CD_3)_3AuPPh_3 \xrightarrow[\text{decalin}]{80\ ^\circ C} CD_3AuPPh_3 + CD_3CD_3 \quad (6)$$

Solutions of an equimolar mixture of $(CH_3)_3AuPPh_3$ and $(CD_3)_3AuPPh_3$ in various solvents were heated in sealed ampoules in vacuo. The decomposition was carried out to low conversions (<20%) in order to minimize complications from further reactions, and the mixture of the isotopically labeled ethanes were determined quantitatively by mass spectral analysis described in the Experimental Section. The results in Table I show that substantial amounts of crossover product (CH_3CD_3) are formed when decompositions were carried out in decalin, chlorobenzene, or ethereal solvents. The extent of crossover in eq 7b is dependent on the absolute concentration of the trimethylgold complexes. Thus, the scrambling of methyl groups approaches the statistical ratio for CH_3CH_3:CH_3CD_3:CD_3CD_3 of 1:2:1 at the relatively high concentration

$$(CH_3)_3AuPPh_3 + (CD_3)_3AuPPh_3 \longrightarrow \begin{cases} CH_3CH_3 + CH_3AuPPh_3 & (7a) \\ CH_3CD_3 + [CH_3AuPPh_3 + CD_3AuPPh_3] & (7b) \\ CD_3CD_3 + CD_3AuPPh_3 & (7c) \end{cases}$$

of 0.15 M. The scrambling diminishes with concentration, as expected, but even in 0.0005 M solutions, roughly 50% of the methyl groups are scrambled during reductive elimination. Control experiments indicate that scrambling in the products is possible from a secondary reaction since a mixture of $(CH_3)_3AuPPh_3$ and CD_3AuPPh_3 afforded CH_3CH_3, CH_3CD_3, and CD_3CD_3 under similar conditions. However, scrambling is more likely to occur between $(CH_3)_3AuPPh_3$ and $(CD_3)_3AuPPh_3$ directly, since no intermolecular exchange was observed in the mixture of methylgold complexes reisolated from a decomposition carried to partial completion (Table I).

Significantly, in polar solvents such as dimethyl sulfoxide (Me_2SO) and dimethylformamide (DMF), the decomposition of a mixture of $(CH_3)_3AuPPh_3$ and its perdeuterated analogue $(CD_3)_3AuPPh_3$ afforded CH_3CH_3 and CD_3CD_3, with only trace amounts of CH_3CD_3, the crossover product. Moreover, reductive elimination of $(CH_3)_3AuPPh_3$ in the presence of CD_3AuPPh_3 afforded only CH_3CH_3 and no CH_3CD_3 or CD_3CD_3 in Me_2SO solutions.

The concentration and solvent dependence of the isotopic composition of ethane formed during reductive elimination suggests the participation of an intermolecular process leading to the scrambling of methyl groups, as well as an intramolecular process in which no scrambling takes place. The intermolecular process for reductive elimination can be formulated as shown in Scheme I. The dissociative step in eq 8 follows from

Scheme I. Intermolecular Processes

$$(CH_3)_3AuL \rightleftharpoons (CH_3)_3Au + L \quad (8)$$

$$(CH_3)_3Au + (CD_3)_nAuL \longrightarrow (CH_3)_3Au(CD_3)_nAuL \quad (9)$$

$$(CH_3)_3Au(CD_3)_nAuL \longrightarrow [CH_3CH_3 + CH_3CD_3 + CD_3CD_3]$$

etc. (10)

the phosphine dependence in the kinetics to be described later (vide infra). According to Scheme I, the coordinatively unsaturated intermediate $(CH_3)_3Au$ associates preferentially with methylgold species (n = 1 or 3) in eq 9, especially in poorly coordinating solvents such as decalin. Reductive elimination from the binuclear gold intermediate in eq 10 leads to methyl scrambling in the ethane, and it must be faster than redissociation since no intermolecular exchange of methyl groups is observed between $(CH_3)_3AuL$ and $(CD_3)_3AuL$.

The intermediate, $(CH_3)_3Au$, however, can be effectively intercepted by better coordinating solvents such as Me_2SO and DMF in eq 11

$$(CH_3)_3Au + S \rightleftharpoons (CH_3)_3AuS \rightarrow CH_3CH_3 + CH_3AuS \text{ etc.} \quad (11)$$

$$S = Me_2SO, DMF, \text{ etc.}$$

to afford labile complexes from which reductive elimination occurs by an intramolecular pathway without scrambling the methyl groups in the product (Table I and vide infra).

If the scrambling results in Table I are interpreted on the basis of Scheme I and eq 11, we deduce that solvents follow the order: Me_2SO > DMF > THF > n-Bu_2O ~ PhCl ~ decalin, in their ability to coordinate with $(CH_3)_3Au$. A similar solvent trend has been observed with $dpyNiEt_2$.[7] Intramolecular studies to be described in the following section relate reductive elimination to cis–trans isomerization in these complexes.

Table II. Thermal Decomposition of *cis*- and *trans*-$CD_3Me_2AuPPh_3$[a]

CD_3Me_2AuL (mg)	Concn (mM)	Solvent	Time (min)	Evolved gas (%) C_2D_6	CH_3CD_3	C_2H_6
		cis-$CD_3Me_2AuPPh_3$				
190[b]	380	PhCl	30	6	44	49
89	180	C_6H_6	20	5	46	49
25	10	$C_{10}H_{18}$	10	5	63	32
25	2.5	$C_{10}H_{18}$	2	4	63	33
13	0.5	$C_{10}H_{18}$	15	6	62	34
25[c]	2.5	Me_2SO	10	0	75	25
		trans-$CD_3Me_2AuPPh_3$				
195[d]	390	PhCl	10	6	46	47
100	200	*t*-BuPh	5	6	50	44
25	170	$C_{10}H_{18}$	5	6	43	51
25	2.5	$C_{10}H_{18}$	2	7	65	28
12.5	0.5	$C_{10}H_{18}$	15	6	64	30
138	270	C_6H_6	5	4	54	42
138	270	C_6H_6	60	9	45	46
25[c]	2.5	Me_2SO	10	0	76	24
96[e]	19	Me_2SO	20	0	75	25

[a] At 80 °C. Observed isomerization of recovered complex: [b] 7%; [c] 100%; [d] 5%. [e] Contains 10 mg of PPh_3, isomerized to 100% for 4 h in C_6H_6, gold complexes reisolated, dissolved in Me_2SO, and decomposed at 100 °C for 20 min.

B. Intramolecular Studies of the Reductive Elimination of $CD_3(CH_3)_2AuL$. The thermal decomposition of pure *cis*-$CD_3(CH_3)_2AuL$ in decalin, chlorobenzene, benzene, *tert*-butylbenzene or di-*n*-butyl ether solution afforded a mixture of protio- and deuterioethanes in amounts corresponding to an almost random coupling of methyl groups [i.e., CH_3CH_3:CH_3CD_3:CD_3CD_3 = 4:4:1] as shown in Table II. Essentially the same mixture of ethanes was obtained from *trans*-$CD_3(CH_3)_2AuL$ under equivalent conditions. It is noteworthy that the unreacted $CD_3(CH_3)_2AuL$ was not isomerized after recovery from the partial decomposition of either the cis or the trans isomer. The distribution of normal and deuterated ethanes in Table II arising from the decomposition of both *cis*- and *trans*-$CD_3(CH_3)_2AuL$ in dilute decalin solutions is thus consistent with the participation of intermolecular routes in the reductive elimination, as found in the studies described above with $(CH_3)_3AuPPh_3$ and $(CD_3)_3AuPPh_3$.

The singular absence of CD_3CD_3 when the decomposition of either *cis*- or *trans*-$CD_3(CH_3)_2AuL$ is carried out in Me_2SO solutions confirms the high degree of reductive elimination proceeding via an intramolecular mechanism in this solvent (cf. eq 11). The liberated ethane consisted of a mixture of only CH_3CD_3 and CH_3CH_3 in a roughly 2:1 ratio. Under these conditions the recovered $CD_3(CH_3)_2AuL$, reisolated after partial decomposition of either the cis or the trans isomer, was completely isomerized. Significantly, there was no intermolecular exchange of methyl groups in the recovered starting materials. Thus, solvents such as Me_2SO effectively suppress the intermolecular reactions observed in others such as decalin, with lower coordinating ability. The latter also coincides with the observation of a facile cis-trans isomerization of $CD_3(CH_3)_2AuPPh_3$ in Me_2SO solutions under conditions in which slow isomerization is observed in chlorobenzene. For example, *cis*-$CD_3(CH_3)_2AuPPh_3$ is 50% isomerized in Me_2SO within 2 h at room temperature (no reductive elimination). The addition of PPh_3 retards isomerization in Me_2SO, an observation which is similar to the results in decalin and benzene solutions described above.

We deduce from the observations in Me_2SO solutions that both intramolecular processes leading to cis-trans isomerization and reductive elimination proceed via a common three-coordinate intermediate previously formulated in Scheme I and included in the mechanism below. The ready

Scheme II. Intramolecular Processes

$$cis\text{-}CD_3(CH_3)_2AuL \rightleftharpoons cis\text{-}CD_3(CH_3)_2Au + L \quad (8)$$

$$cis\text{-}CD_3(CH_3)_2Au \rightleftharpoons trans\text{-}CD_3(CH_3)_2Au \quad (12)$$

$$cis,trans\text{-}CD_3(CH_3)_2Au + S \rightleftharpoons cis,trans\text{-}CD_3(CH_3)_2AuS \quad (13)$$

$$cis,trans\text{-}CD_3(CH_3)_2Au \rightarrow CD_3CH_3 + CH_3CH_3, \text{etc.} \quad (14)$$

$$cis,trans\text{-}CD_3(CH_3)_2Au \xrightarrow{L} cis,trans\text{-}CD_3(CH_3)_2AuL \quad (15)$$

cis-trans isomerization of $CD_3(CH_3)_2AuPPh_3$ obtained in Me_2SO precludes any stereochemical information regarding the reductive elimination in eq 14 in this solvent.

Ligand Effects in Ethyldimethyl(triphenylphosphine)gold: Kinetics of Cis–Trans Isomerization and Reductive Elimination. Pure *cis*-$Et(CH_3)_2AuPPh_3$ in benzene solution undergoes a simultaneous reductive elimination and cis-trans isomerization at 70 °C. However, the addition of small amounts of triphenylphosphine strongly retards the reductive elimination, allowing the cis-trans isomerization to be examined separately.

Cis–Trans Isomerization. The rate of isomerization of *cis*-$Et(CH_3)_2AuPPh_3$ at various concentrations in benzene solutions at 70 °C follows first-order kinetics. (The equilibrium mixture at this temperature contains 70% of the trans isomer, i.e., K = 2.3.)

$$\begin{matrix} CH_3 \\ | \\ CH_3AuPPh_3 \\ | \\ Et \end{matrix} \overset{K}{\rightleftharpoons} \begin{matrix} CH_3 \\ | \\ EtAuPPh_3 \\ | \\ CH_3 \end{matrix} \quad (16)$$

The rate of isomerization of *cis*-$Et(CH_3)_2AuPPh_3$ is retarded by added PPh_3. The reciprocal of the pseudo-first-order rate constant k_{ct} shown in Figure 1 varies linearly with the concentration of added PPh_3. However, the magnitude of the retardation is not large as indicated by the relatively small changes in k_{ct} with increasing concentrations of PPh_3 in Table III.

The ^{31}P NMR spectrum of $Et(CH_3)_2AuPPh_3$ in benzene solutions shows only the resonance due to coordinated PPh_3 at δ109 ppm, indicating no significant dissociation of the ligand. With increasing amounts of added PPh_3, the chemical shift of the coordinated PPh_3 remains more or less invariant but the half-width of the resonance broadens as shown in Table

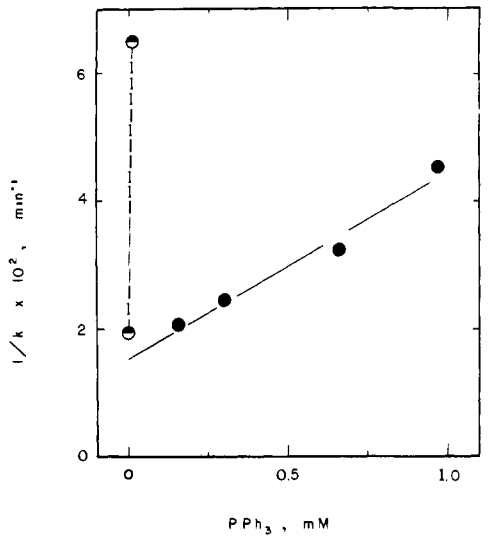

Figure 1. Effect of added PPh_3 on the rate of cis-trans isomerization ● and reductive elimination ⊖ of *cis*-$Et(CH_3)_2AuPPh_3$ in benzene.

IV. The accompanying resonance due to free added PPh_3 is not broadened perceptibly. Furthermore, the absence of additional ^{31}P resonances indicates that the concentration of a five-coordinate intermediate[8a] such as $Et(CH_3)_2Au(PPh_3)_2$, even at the highest concentrations of PPh_3 studied, is small. We attribute the selective line broadening to an associative exchange of the ligand in eq 17,

$$Et(CH_3)_2AuPPh_3 + PPh_3 \rightleftharpoons Et(CH_3)_2Au(PPh_3)_2 \quad (17)$$

the equilibrium constant of which is too small to measure by our NMR techniques.

The associative exchange of PPh_3 as described in eq 17, however, is not directly related to the cis-trans isomerization of $Et(CH_3)_2AuPPh_3$. Thus trimethylphosphine and dimethylphenylphosphine are several orders of magnitude more effective than triphenylphosphine in retarding the rate of isomerization (Table V). Examination of the proton NMR spectrum clearly shows that phosphine exchange in eq 18 takes place readily on mixing, e.g.,

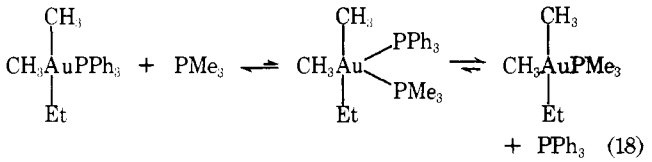

(18)

but it occurs *without* cis-trans isomerization (see Experimental Section).[8b] The exchange is too fast and stereospecific to proceed via a dissociative mechanism. Thus, ligand exchange and cis-trans isomerization are largely independent processes, the former occurring by an associative mechanism and the latter by a dissociative pathway. Moreover, species such as $Et(CH_3)_2AuL_2$ formed in the associative exchange are not present in sufficient concentrations to be kinetically important either in cis-trans isomerization or reductive elimination, and will be ignored in discussions hereafter.

Reductive Elimination. The reductive elimination of *cis*-$Et(CH_3)_2AuPPh_3$ is more effectively retarded by PPh_3 than cis-trans isomerization (Table III). In the absence of any added PPh_3, the reductive elimination of *trans*-$Et(CH_3)_2AuPPh_3$ in decalin solutions produced mainly propane whereas the cis isomer afforded a mixture of ethane and propane. Earlier we deduced[2] from these and similar results that reductive elimination proceeded by loss of cis-alkyl groups from a T-shaped three-coordinate intermediate, and it occurred

Table III. Rates of Isomerization and Reductive Elimination of *cis*-$EtMe_2AuPPh_3$.[a] Effect of Added Triphenylphosphine

$EtMe_2AuL$ (10 M)	Ph_3P (10 M)	k_{ct} (10^4 s^{-1})	k_{re} (10^4 s^{-1})
0.099	0	*b*	0.88
0.099	0.095	*b*	0.26
2.7	0	1.0[c]	
2.7	1.5	0.81	
1.3	1.5	0.80	
2.7	3.0	0.68	
2.7	6.6	0.52	
2.7	9.7	0.37	

[a] In benzene at 70 °C in vacuo. [b] Not measured due to simultaneous decomposition. [c] Calculated from the intercept in Figure 1.

Table IV. ^{31}P NMR Parameters of *cis*-$EtMe_2AuPPh_3$[a]

$EtMe_2AuP$-Ph_3 (10^2 M)	PPh_3 (10^2 M)	^{31}P parameters[b] $AuPPh_3$ δ (ppm)	$AuPPh_3$ Δν (Hz)	PPh_3(free) δ (ppm)	PPh_3(free) Δν (Hz)
0.13	0	108.9	1.4		
0.13	0.15	108.7	2.2	141.6	8.5
0.13	0.66	108.7	3.6	142.2	8.4
0	0.2			142.6	1.7

[a] In benzene at 70 °C. [b] Line width at half height, chemical shift relative to external $P(OMe)_3$, upfield is positive. Proton decoupled. Resolution is ±0.6 Hz (proton decoupled).

Table V. Kinetics of Cis-Trans Isomerization of *cis*-$EtMe_2AuPPh_3$[a]

$EtMe_2AuL$ L	(M)	Additive L′	(M)	k_{ct} (s^{-1})
PPh_3	(0.20)	0		1.0×10^{-4} [b]
PPh_3	(0.22)	PMe_3	(0.42)	$<10^{-7}$ [c]
PPh_3	(0.16)	PMe_2Ph	(0.29)	$<10^{-7}$ [d]
PMe_2Ph	(0.25)	0		0.27×10^{-4}
PMe_2Ph	(0.25)	PMe_2Ph	(0.50)	$<10^{-7}$
PMe_3	(0.30)	0		0.22×10^{-4}
PMe_3	(0.30)	PMe_3	(0.40)	$<10^{-7}$
PMe_3	(0.30)	PPh_3	(0.80)	0.13×10^{-4}

[a] In benzene at 70 °C. [b] Calculated from intercept in Figure 1. [c] Only *cis*-$EtMe_2AuPMe_3$ observed. [d] Only *cis*-$EtMe_2AuPMe_2Ph$ observed by proton NMR.

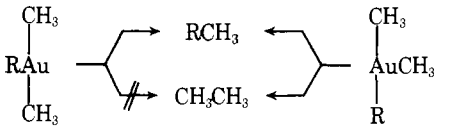

(19)

faster than isomerization under these conditions. As expected, both *cis*- and *trans*-$Et(CH_3)_2AuPPh_3$ afforded the same mixture of ethane and propane in the presence of added PPh_3, since isomerization under these conditions preceded the slower, retarded reductive elimination.

However, the discovery, described above, of an intermolecular route for reductive elimination of $(CH_3)_3AuPPh_3$ in decalin solutions has caused us to question whether the earlier conclusions were obscured by a similar process occurring with $Et(CH_3)_2AuPPh_3$ and its homologues.

We have reconfirmed the earlier results, including the presence of *n*-butane. The latter, albeit in minor amounts, is diagnostic of an intermolecular pathway, especially since it increases with the concentration of $Et(CH_3)_2AuPPh_3$ (Table

Table VI. Thermal Decomposition of *cis*- and *trans*-$EtMe_2AuPPh_3$

$EtMe_2AuPPh_3$ (10 M)	PPh_3 (10 M)	Solvent	Temp (°C)	Alkane (%) C_2H_6	C_3H_8	n-C_4H_{10}
Trans (0.14)[a]	0	$C_{10}H_{18}$	70	3	94	2
Cis (0.088)[a]	0	$C_{10}H_{18}$	70	32	64	4
Trans (1.85)	0	$C_{10}H_{18}$	80	13	76	11
Trans (0.099)	0	Me_2SO	80	8	91	1
Cis (0.099)	0	Me_2SO	80	5	88	6
Trans (0.098)[a]	(0.11)	$C_{10}H_{18}$	90	2	96	2
Cis (0.11)[a]	(0.11)	$C_{10}H_{18}$	90	3	95	2

[a] Taken from ref 2. $C_{10}H_{18}$ = decalin.

VI). Due to the differences in chemical properties of ethyl and methyl groups, the data do not allow the extent of intermolecular pathways to be evaluated for $Et(CH_3)_2AuPPh_3$, nor can the foregoing results derived from $CD_3(CH_3)_2AuPPh_3$ be applied quantitatively to this homologue. Thus, the stereochemical conclusions regarding reductive elimination from the three-coordinate intermediate in eq 19 appear to be premature at this juncture.[33] Furthermore, despite the absence of termolecular reactions in Me_2SO solutions, stereochemical information regarding the reductive elimination of $Et(CH_3)_2AuPPh_3$ cannot be obtained under these conditions due to the rapid cis-trans isomerization which causes the same mixture of dimer alkanes to be produced (Table VI) from both isomers.

The Mechanism of Cis-Trans Isomerization and Reductive Elimination. Both intramolecular processes leading to cis-trans isomerization and reductive elimination of trialkyl(phosphine)gold complexes occur by dissociative mechanism involving the prior loss of phosphine ligand. A mechanism is presented in Scheme III which incorporates the results on hand and interrelates cis-trans isomerization with reductive elimination via common intermediates. According to Scheme III,

Scheme III. Intramolecular Cis-Trans Isomerization and Reductive Elimination

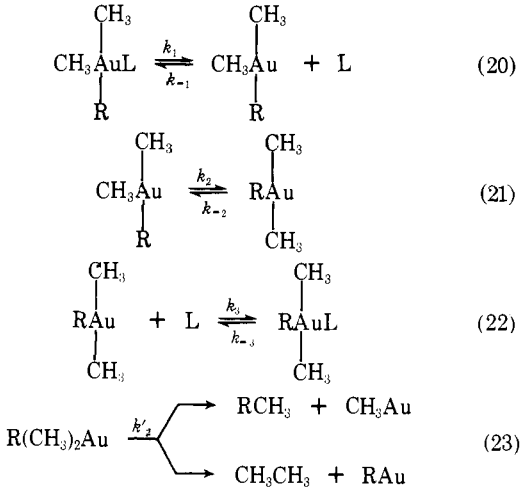

cis-trans isomerization and reductive elimination proceed from the three-coordinate intermediate RMe_2Au. Since the isomerization could be studied separately, it will be first described independently.

Cis-Trans Isomerization. The rate of isomerization of *cis*-$Et(CH_3)_2AuPPh_3$, I(R = Et), is given by eq 24, if we employ the mechanism in Scheme III and the steady-state approximation,

$$\frac{-d(I)}{dt} = \frac{[k_1k_2k_3 + k_{-1}k_{-2}k_{-3}](I)}{k_{-1}k_{-2} + k_2k_3 + k_{-1}k_3(PPh_3)} = k_{ct}(I) \quad (24)$$

where k_{ct} is the experimental pseudo-first-order rate constant for isomerization and $(I) = (I)_t - (I)_{equil}$. The form of eq 24 agrees with the experimental results in which the reciprocal of k_{ct} is proportional to (PPh_3).

$$\frac{1}{k_{ct}} = \frac{k_{-1}k_{-2} + k_2k_3 + k_{-1}k_3(PPh_3)}{k_1k_2k_3 + k_{-1}k_{-2}k_{-3}} \quad (25)$$

The rates of ligand dissociation and association in the cis and trans isomers should be the same, i.e., $k_1 = k_{-3}$ and $k_{-1} = k_3$. If $k_2 = k_{-2}$, eq 25 simplifies to

$$\frac{1}{k_{ct}} = \frac{1}{k_1} + \frac{k_{-1}(PPh_3)}{2k_1k_2} \quad (26)$$

The intercept in Figure 1 is equal to $1/k_1$, or $k_1 = 1.0 \times 10^{-4}$ s^{-1}. The slope, which reflects retardation by PPh_3, is given by $k_{-1}/2k_1k_2$, and its magnitude (1.7×10^4 s M^{-1}), indicates that k_{-1} is comparable to k_2. Specifically, the rate of isomerization of the three-coordinate intermediate in eq 21 is 34 times slower than reassociation in a 0.1 M solution of PPh_3. The absolute rate of reassociation can be obtained from the equilibrium constant, $K = k_1/k_{-1}$. Although K is not accurately known, on the basis of molecular weight (vapor pressure osmometry) and $^1H/^{31}P$ NMR studies, we estimate that $K < 10^{-3}$ M, from which $k_{-1} > 10^{-1}$ M^{-1} s.[9]

Reductive Elimination. Proceeding again from Scheme III and employing the steady-state approximation, the rate of reductive elimination from *cis*- and *trans*-$Et(CH_3)_2AuPPh_3$, I′, is given by:

$$\frac{-d(I')}{dt} = \frac{k_1k'_2(I')}{k_2 + k_{-1}(PPh_3)} \quad (27)$$

and

$$\frac{1}{k_{re}} = \frac{1}{k_1} + \frac{k_{-1}(PPh_3)}{k_1k'_2} \quad (28)$$

where k_{re} is the experimental pseudo-first-order rate constant for reductive elimination and the other rate constants are those in Scheme III.[10] Due to complications arising from further decomposition of alkylgold(I) products in benzene solutions (vide supra), the reductive elimination does not follow pseudo-first-order kinetics to high conversions. If we employ only the initial rates in the determination of k_{re}, we obtain $k_1 = 0.88 \times 10^{-4}$ s^{-1} in Table III, which is in reasonable agreement with the value determined from the kinetics of cis-trans isomerization. From the slope in Figure 1, we obtain $k_{-1}/k_1k'_2 = 3 \times 10^6$ s M^{-1} compared to $k_{-1}/2k_1k_2 = 1.7 \times 10^4$ s M^{-1} for isomerization, or $k_2/k'_2 \sim 10^2$. In other words, cis-trans isomerization of the T-shaped three-coordinate intermediate in eq 21 proceeds roughly one hundred times faster than reductive elimination in eq 23.

The kinetics derived from Scheme III are generally applicable to cis-trans isomerization and reductive elimination taking place in more or less innocent solvents, such as decalin and benzene. In Me_2SO solvent, however, the association of the three-coordinate intermediate must be included,

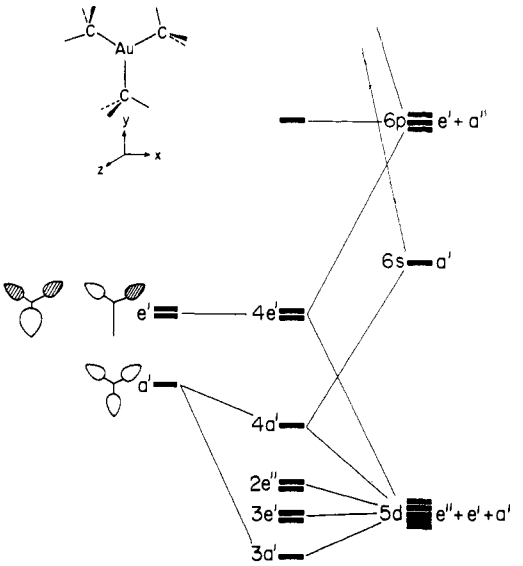

Figure 2. Interaction diagram for trimethylgold in C_{3h} symmetry. The coordinate system is shown in the upper left corner. The important orbitals of the trimethyl fragment (neglecting the hydrogens) are drawn on the left.

$$R(CH_3)_2Au + S \underset{k_4}{\overset{k_{-4}}{\rightleftharpoons}} R(CH_3)_2AuS \qquad (29)$$

and the rate constant for isomerization k_{ct} becomes:[11]

$$\frac{1}{k_{ct}} = \frac{1}{k_1} + \frac{k_{-1}(PPh_3)}{2k_1k_2} + \frac{k_{-4}(S)}{2k_1k_2} \qquad (30)$$

and that for reductive elimination k_{re} is:

$$\frac{1}{k_{re}} = \frac{1}{k_1} + \frac{k_{-1}(PPh_3)}{k_1k'_2} + \frac{k_{-4}(S)}{k_1k'_2} \qquad (31)$$

Equations 30 and 31 differ from 26 and 28, respectively, only by added solvent terms. In the absence of added phosphine, the rates of isomerization and reductive elimination are no longer the same, as they are in benzene, but depend on the relative magnitudes of k_2 and k'_2. Indeed, in Me_2SO solutions without added PPh_3, the observation of a faster rate of cis-trans isomerization compared to reductive elimination of Et-$(CH_3)_2AuPPh_3$ follows from the result that $k_2/k'_2 \sim 10^2$, since both being unimolecular processes should be rather insensitive to solvent effects (i.e., Me_2SO compared to benzene).

The Three-Coordinate Intermediate, $R(CH_3)_2Au$—Reductive Elimination and Isomerization. In view of the faster rate of isomerization, neither kinetic nor product analysis can be used to rigorously deduce the stereochemistry of reductive elimination from the three-coordinate trialkylgold intermediate. In order to investigate further the potential energy surface and the stereochemistry for reductive elimination from this reactive intermediate, we have carried out molecular orbital calculations of $(CH_3)_3Au$, particularly with regard to T- and Y-shaped configurations.

We begin with a highly symmetrical C_{3h} configuration of trimethylgold, analogous to III. Figure 2 shows an interaction

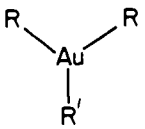

III.

diagram for this structure. At the right are the metal orbitals and at the left the orbitals of the three interacting methyl groups. The a' + e' methyl set is composed of the CH_3 radical a_1 orbitals.[12] In $(CH_3)_3Au$ there are 14 electrons to be placed into the levels shown. The result is a half occupied 4e' level, with the immediate implication that the system is Jahn-Teller unstable. A distortion is indicated, shown in IV and V, to either T- or Y-shaped geometries of lower symmetry.[13]

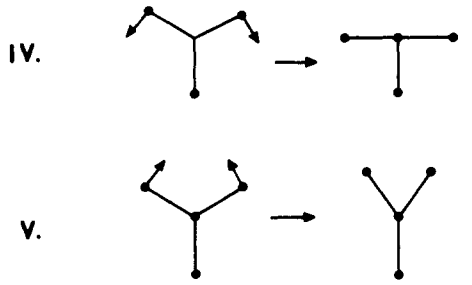

This distortion is traced in full detail as follows. The 4e' orbital is built up from a linear combination of the e' combination of methyl radical lobes and gold xy and $x^2 - y^2$.[14] The mixing is out-of-phase since the methyl orbitals are of higher energy than the metal 5d set. There is also a significant incorporation of metal x,y, which also transform as e'. The phase of this mixing, a polarization phenomenon, is easily predicted from a second-order perturbation theory argument,[15] and yields the final shape of the 4e' set shown in VI and VII.

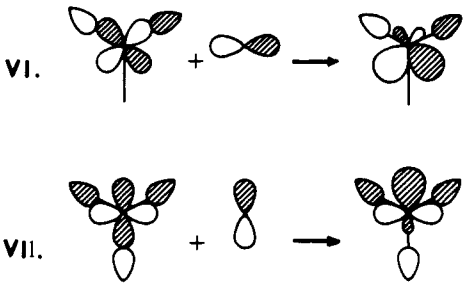

Distortion of VI to a T geometry will stabilize this level since the ligand orbitals move into the node of the gold xy and become strongly bonding with the gold x orbital. This same distortion destabilizes VII since the methyl orbitals move into the node of the bonding gold y orbital and become strongly antibonding with $x^2 - y^2$. Distortion to a Y geometry will have exactly the opposite effect on splitting the 4e' set; VI becomes destabilized and VII stabilized.

A Walsh diagram for the deformation to either T or Y shapes is given in Figure 3 (top). In addition to the clearly defined splitting of 4e' the charges in the other valence levels are also indicated. The 3a' and 4a' levels are symmetric and antisymmetric combinations, respectively, of gold z^2 mixing with methyl hybrid orbitals directed toward the gold atom (see Figure 2). These levels, as expected, vary only slightly with the C-Au-C angle α. The 2e'' set is essentially xz and yz orbitals on gold, and therefore is again rather insensitive to α. The 3e' levels are comprised of gold xy and $x^2 - y^2$. They split in a fashion analogous to that described for the 4e' set. Finally there is the 2a' orbital, which was omitted from the interaction diagram of Figure 2, but lies directly below in energy. The 2a', shown schematically in VIII, is descended from a linear com-

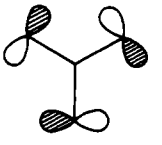

VIII.

bination of hyperconjugating π-type orbitals of a CH_3 group.[12] This orbital will figure below in the discussion of the reductive

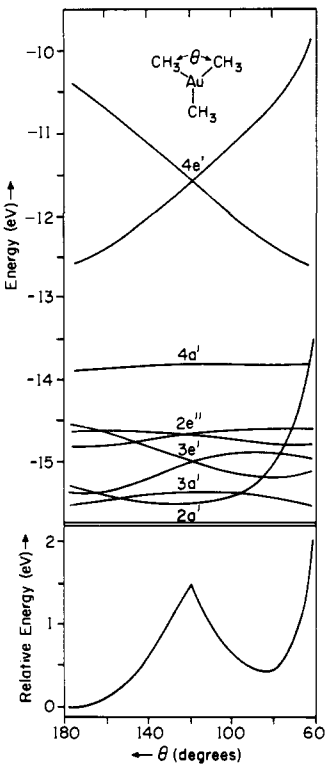

Figure 3. Top: A Walsh diagram for the valence levels of $Au(CH_3)_3$ as a function of the distortion angle θ. Bottom: Total energy for $Au(CH_3)_3$ as a function of θ.

elimination of ethane. In Figure 3a it may be seen that it is this orbital which is in large part responsible for the destabilization of the Y configuration of trimethylgold relative to that of the T.

It is clear that $(CH_3)_3Au$ will distort spontaneously from the threefold symmetric geometry III to T and Y shapes. Of course there are three ways in which each of these lower symmetry conformations may be reached. Scheme IV summarizes the totality of R_3Au deformations, and Figure 4 elaborates on this schematic picture by showing a potential energy surface in which the two independent C-Au-C angles, α and β, are scanned.

Scheme IV

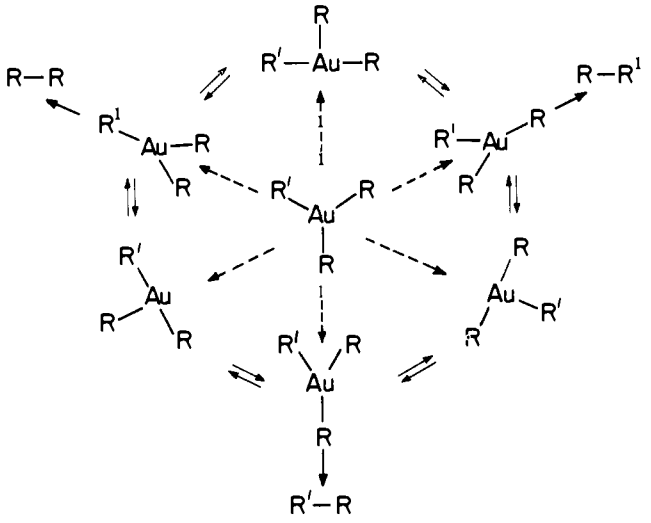

The surface of Figure 4 is hardly novel, since it will always be generated for a molecule possessing a threefold symmetry axis with a Jahn-Teller instability.[13b,16] Thus, two such surfaces have been encountered before, one in a study of the re-

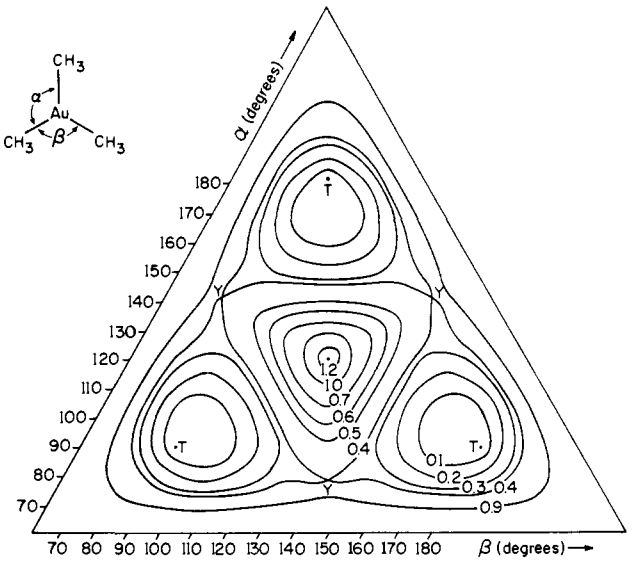

Figure 4. Computed surface for variation of the two C-Au-C angles, α and β, in trimethylgold. The energies are in electron volts relative to the T configuration.

arrangements of $(CH)_5^+$ [17] and the other in an ab initio study of LiH_3.[18,19] The D_{3h} geometry of this six-electron molecule has the configuration $(1a')^2(2a')^2(e')^2$,[20] and deformation to T and Y minima was favored.[21] Moreover, the Y configurations acted as exit channels for the elimination of H_2, which is similar to that suggested for trimethylgold in this study.

The basic feature of the potential energy surface for trialkylgold complexes is set by the orbital degeneracy on the C_{3h} geometry. That symmetric geometry is a high point in energy. Surrounding it is a girdle of lower energy conformations containing three equivalent T-shaped minima and three equivalent Y-shaped saddle points. These Y-shaped geometries serve as exit channels for the elimination of the coupled alkane.

At first sight it would appear as though the Y geometries serve as the meeting points of three valleys—two leading to the more stable T shapes and one leading to reductive elimination. Such a description is tantamount to the "monkey saddle" problem, elegantly analyzed by McIver and Stanton.[22] In fact the surface is not two-dimensional, as expected in Figure 4, but must include methyl rocking off the Au-C axis and differential Au-C elongations. Distinct transition states for cis-trans isomerization of T to T′ and reductive elimination of T indeed exist. Both processes will have their saddle points in a region in which the C_3Au skeleton has the rough appearance of a Y, and so, while cognizant of the difference, they will both be described loosely as Y.

A correlation diagram for the reductive elimination of ethane from a Y geometry of trimethylgold is shown in Figure 5. The orbitals are classified as symmetric (S) or antisymmetric (A) with respect to a pseudo-mirror plane shown in IX.[23,24]

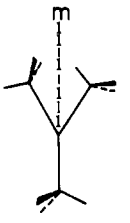

IX.

The elimination of ethane is clearly a symmetry-allowed process. A similar conclusion, using the methodology introduced

Table VII. Scrambling in the Coupling of Lithium Dimethylmetalates (Me_2MLi) with Methyl Derivatives (RX)[a]

Me_2MLi	MX (mmol)	CD_3Li (mmol)	MeLi (mmol)	RX (mmol)	Ethanes (%) C_2D_6	CH_3CD_3	C_2H_6
$CH_3(CD_3)CuLi$[b]	CuI (0.44)	0.47	0.63	CH_3I (1.19)	0	33	67
$CH_3(CD_3)CuLi$[b]	CuI (0.44)	0.47	0.63	CH_3Tf (0.46)	0	34	66
$(CH_3)_2CuLi$	CuI (1.00)	0	2.00	CD_3I (0.79)	0	96	4
$CH_3(CD_3)CuLi$[b]	CuI (0.44)	0.47	0.63	O_2 (0.5)	11	46	44
$(CH_3)_2AuLi$	AuCl (0.99)	0	2.00	CD_3I (0.79)	16	53	31

[a] In Et_2O, see Experimental Section for details. [b] Assuming no isotope effect in equilibria.

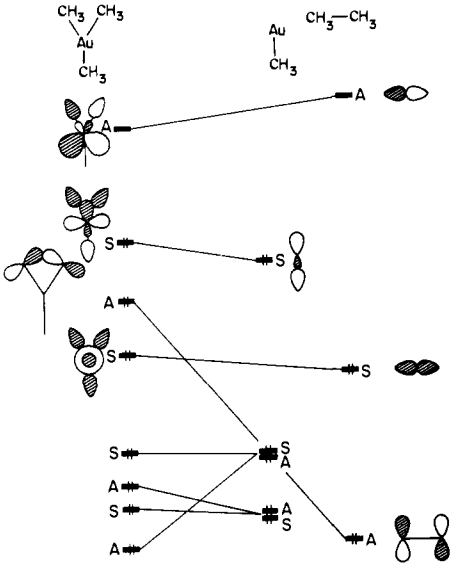

Figure 5. Correlation diagram for the elimination of ethane from trimethylgold. The energy levels for the trimethylgold correspond to those in Figure 3 with $\theta = 60°$. The hydrogens have been left out for convenience.

by Pearson,[25] has been reached by Brown, Puddephatt, and Upton,[26] in a mechanistic analysis of the related reductive elimination of ethane from trialkyl-Pt(IV) complexes.

Given that the elimination of ethane is an allowed process, we were interested in obtaining a rough theoretical estimate of the activation energy. Usually the extended Hückel procedure would not be the method of choice for this type of problem, since it does not account well for molecular deformations involving bond stretching. In the case at hand we were encouraged by the fact that bond length optimization in $(CH_3)_3Au$ for the T geometry yielded a reasonable value of 2.05 Å for the bond length for Au-C (Note: Observed Au(I) or Au(III) to C bond lengths lie in the range 1.9-2.2 Å.[27]) but any numerical results presented here should be viewed with caution.

In the process of reductive elimination of ethane from $(CH_3)_3Au$, a dimension that must be added is the rocking of the methyl groups away from the gold, and toward each other as represented in X. At the saddle point corresponding to the

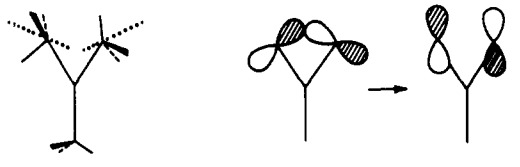

X. XI.

Y conformation in Figure 4, the methyl axes turn by 9.6° away from the Au-C line. The Au-C bond length to the two methyl groups also increases by ~0.05 Å. The rocking motion serves to stabilize the crucial orbital derived from VIII, as shown schematically in XI. Further motions combine C-C bond shortening, C-Au elongation, and methyl reorientation (a continuation of the rocking motion). The calculated transition state correspond to the Au-C bond elongated by approximately 0.2 Å, the C-Au-C angle of 55°, and methyl axes tilted by 38° from C-Au. The computed estimate of the activation energy for ethane elimination is 0.8 eV. Even within the limitations of the approximate MO scheme this is an upper bond, since the position of the methyl group that remains bonded to Au was not optimized nor that of any of the interior coordinates of the idealized CH_3 groups. Interestingly, the calculated activation energy for isomerization from one T structure to another (Figure 4) is near 0.4 eV and less than the computed pass height for elimination, which is consistent with the experimental results described above.

Comments on the Copper(I) Catalyzed Coupling Reaction. Lithium dimethylcuprate(I) reacts rapidly with methyl iodide to produce ethane.[3,28] The same reaction with CD_3I affords CH_3CD_3 in 96% isotopic purity, 4% CH_3CH_3, and no CD_3CD_3. Similarly, the mixed cuprate $CH_3(CD_3)CuLi$ with CH_3I produces a mixture of CH_3CD_3 (33%) and CH_3CH_3 (67%), but no CD_3CD_3. The same results obtain with $CH_3O_3SCF_3$ as shown in Table VII. The coupling reaction with phosphine-free dimethylaurate(I) is also included for comparison.[29]

$$(CH_3)_2CuLi + CD_3I \rightarrow CH_3CD_3 + CH_3Cu + LiI \quad (32)$$

These studies clearly demonstrate that the copper(I) catalyzed coupling reaction between dimethylcuprate and methyl iodide or triflate proceeds specifically with no exchange of methyl groups. Mechanistically, it is possible for the coupling to proceed directly via a four-center transition state or in two steps, first oxidative addition to a trimethylcopper(III) intermediate followed by reductive elimination.[28,30] Both are consistent with the deuterium labeling studies. The latter bears direct similarity to the process described above for the gold analogues. If the two-step mechanism also applies to copper, we deduce that reductive elimination proceeds by cis elimination from a T-shaped trimethylcopper intermediate, as described in Scheme IV for gold.[31]

Summary and Conclusions

Isomerization and reductive elimination in a series of cis and trans trialkyl(phosphine)gold complexes ($R(CH_3)_2AuL$, where R = CH_3, CD_3, and CH_3CH_2, and L = PPh_3, PMe_3, and PMe_2Ph) have been studied by the isotopic analysis of the products and kinetic dependence on added phosphine. Reductive elimination leading to the scrambling of CH_3 and CD_3 groups in the product arises from an intermolecular process which is important only in nonpolar solvents such as decalin and benzene.[32] Cis-trans isomerization in these solvents does not proceed via an intermolecular process, and the reactants (after partial decomposition) can be recovered intact. Only intramolecular processes occur in Me_2SO and DMF solutions since no exchange is observed during either cis-trans isomer-

Table VIII. ^1H NMR Spectra of Trialkylgold Complexes, $R_3AuPR'_3$[a]

R_3AuL	Solvent	trans-Me δ	trans-Me J_{H-P}	cis-Me δ	cis-Me J_{H-P}	Et δ	Et J_{H-P}	PR'_3 δ	PR'_3 J_{H-P}
Me_3AuPPh_3	C_6H_6	1.83 (3 H)	9	0.68 (6 H)	8			[b]	
Me_3AuPPh_3	Diox[c]	0.87 (3 H)	9.3	0.23 (6 H)	7.2			7.27 (15 H)	m
Me_3AuPPh_3	$CDCl_3$	1.10 (3 H)	9	0.03 (6 H)	7			7.2–7.8 (15 H)	
Me_3AuPMe_3	Diox[c]	0.89 (3 H)	9.7	0.04 (6 H)	7.8			0.42 (9 H)	
Me_3AuPMe_2Ph	CH_2Cl_2	0.87 (3 H)	9	0.07 (6 H)	7			1.77 (6 H)	10
								7.2–7.8 (5 H)	
cis-$(CD_3)Me_2AuPPh_3$	C_6H_6	1.83 (3 H)	9	0.68 (3 H)	8			[b]	
trans-$(CD_3)Me_2AuPPh_3$	C_6H_6	1.83 (0 H)	9	0.68 (6 H)	8			[b]	
$(CD_3)_3AuPPh_3$	C_6H_6	—		—				[b]	
cis-$EtMe_2AuPPh_3$	C_6H_6	1.73 (3 H)	9	0.53 (3 H)	7	1.2–1.4 (5 H)	m	[b]	
trans-$EtMe_2AuPPh_3$	C_6H_6	—		0.65 (6 H)	7	1.2–2.5 (5 H)	m	[b]	
cis-$EtMe_2AuPMe_3$	C_6H_6	1.48 (3 H)	9	0.52 (3 H)	8	1.0–1.9 (5 H)	m	0.88 (9 H)	9.2
trans-$EtMe_2AuPMe_3$	C_6H_6	—		0.59 (6 H)	8	1.0–2.5 (5 H)	m	0.85 (9 H)	9.2
cis-$EtMe_2AuPPhMe_2$	C_6H_6	1.60 (3 H)	9	0.58 (3 H)	8	1.0–1.9 (5 H)	m	1.18 (6 H)	9.2
trans-$EtMe_2AuPPhMe_2$	C_6H_6	—		0.70 (6 H)	8	1.0–2.5 (5 H)	m	1.15 (6 H)	9.2
cis-$EtMe_2AuPPh_3$ + PMe_3	C_6H_6[d]	1.47 (3 H)	9	0.50 (3 H)	8	1.0–1.9 (5 H)	m	0.88 (9 H)	9.2
								0.88[e]	2
cis-$EtMe_2AuPPh_3$ + PMe_2PPh	C_6H_6[d]	1.60 (3 H)	9	0.58 (3 H)	8	1.0–1.9 (5 H)	m	1.24 (6 H)	9.2
								1.10[f]	4

[a] Chemical shifts (ppm) relative to benzene (δ 7.27), others relative to Me_4Si (internal standard), m = unresolved multiplet, doublet coupling constants in Hz. [b] Obscured by solvent. [c] From ref 8a, diox = 1,4-dioxane. [d] Spectrum taken immediately after mixing. [e] Free PMe_3. [f] Free PMe_2Ph.

ization or reductive elimination in this solvent. In Me_2SO solutions, reductive elimination occurs more slowly but the rate of isomerization is faster than in benzene. Reductive elimination is more strongly retarded by added phosphine than cis–trans isomerization and allows the latter to be studied independently in benzene solutions. Isomerization of $Et(CH_3)_2AuL$ in the presence of incremental amounts of phosphine follows Michaelis–Menten type of kinetics.

The divers results can be quantitatively interrelated by a simple mechanism outlined in Scheme III involving a single intermediate, a three-coordinate trialkylgold species, R_3Au. Kinetic analysis employing this unified scheme affords a rate-limiting dissociation of phosphine proceeding with a rate constant, $k_1 = 1.0 \times 10^{-4}$ s^{-1} at 70 °C. The reassociation of R_3Au with phosphine is estimated to be $k_1 > 10^{-1}$ M^{-1} s^{-1} from an approximate equilibrium constant, $K < 10^{-3}$ M. Since the unimolecular isomerization (k_2) of the coordinatively unsaturated $Et(CH_3)_2Au$ occurs 100 times faster than reductive elimination (k'_2), its association with solvents such as Me_2SO allows isomerization to take place without reductive elimination (cf. eq 30 and 31). In the absence of coordinating solvents, R_3Au associates with other alkylgold species to form labile binuclear complexes in Scheme I, eq 10, leading to intermolecular scrambling in the products. Since neither kinetic nor product analysis under these circumstances allows an unequivocal assignment of the stereochemistry of reductive elimination,[33] approximate molecular orbital calculations are used to probe the energy surface of the Me_3Au intermediate. The most symmetric configuration (C_{3h}) is Jahn–Teller active, and distortions to T- and Y-shaped geometries of lower energy are favored. Cis–trans isomerization occurs between T-shaped configurations which are energy minima (Figure 4). Y-Shaped configurations are saddle points for isomerization and serve as exit channels for the reductive elimination of ethane as shown in Scheme IV. Rough theoretical estimates of the activation energies for isomerization and reductive elimination are consistent with the kinetic results based on Scheme III.

Experimental Section

Preparation of Trialkylgold Complexes. *cis*- and *trans*-$Et(CH_3)_2AuPPh_3$ and $(CH_3)_3AuPPh_3$ were prepared as reported previously.[2]

***cis*-$CD_3(CH_3)_2AuPPh_3$.** CD_3MgI (from 200 mg of Mg and 0.5 ml of CD_3I in Et_2O) was added dropwise to an ethereal suspension of $(CH_3)_2AuIPPh_3$ (816 mg) at 0 °C under Ar. After stirring for 1 h, the ice bath was removed and the reaction stirred for an additional 1 h. The mixture was recooled and distilled water (20 ml) was carefully added. The ether layer was separated and the aqueous solution extracted with *n*-pentane. The combined extract was concentrated in vacuo to afford white crystals. Recrystallization from *n*-pentane afforded 200 mg of *cis*-$CD_3(CH_3)_3AuPPh_3$. Its isotopic purity was determined by NMR analysis using as calibration curves the areas of the cis and trans methyl resonances of $(CH_3)_3AuPPh_3$ relative to 1,4-dioxane as an internal standard in $CDCl_3$. The isotopic composition was 98%, with 1.5% $(CH_3)_3AuPPh_3$ and 0.5% of the trans isomer as impurities.

***trans*-$CD_3(CH_3)_2AuPPh_3$.** CD_3I (0.5 ml) was slowly added to a homogeneous solution of $(CH_3)_2AuLiPPh_3$ (obtained from 2.2 g of $AuClPPh_3$ and 5.8 ml of 1.5 M CH_3Li in Et_2O) at 0 °C under Ar. The solution was stirred for 1 h at 0 °C and for additional 1 h at room temperature. Workup and analysis were as described above. Isotopic purity was 87.5%, the impurities being 12% of the cis isomer and 0.5% of $(CH_3)_3AuPPh_3$. A correction for these impurities was made in subsequent studies of reductive elimination.

$(CD_3)_3AuPPh_3$. CD_3Li was prepared from 70 mg of Li metal and 260 μl of CD_3I in 5 ml of Et_2O. It was added to a suspension of $ClAuPPh_3$ (1.0 g) in 15 ml of Et_2O at 0 °C under Ar, and stirred for 1 h at 0 °C. After an additional hour at room temperature, the mixture was cooled in ice and 130 μl of CD_3I added. Workup afforded 350 mg of $(CD_3)_3AuPPh_3$; isotopic purity 99%.

$(CH_3)_3AuPPhMe_2$. The subject compound was prepared by the same procedure described above for $(CD_3)_3AuPPh_3$, using CH_3Li (7.6 ml of 1.5 M solution), 2.1 g of $ClAuPPhMe_2$, and 0.5 ml of CH_3I, to afford a colorless liquid, yield 1.73 g (80%).

***cis*-$Et(CH_3)_2AuPPhMe_2$.** Iodine (1.16 g) was added to 1.73 g of $Me_3AuPPhMe_2$ in dichloromethane at room temperature. The solvent was removed and yellow solid dissolved in Et_2O after drying. EtMgBr (from 1 g Mg and 3 ml of EtBr) was slowly added to the ethereal solution at 0 °C under Ar. Workup yielded 0.80 g (40%) of a colorless liquid.

$(CH_3)_3AuPMe_3$. $AuCl(PMe_3)$ (883.4 mg) was treated with 3.4 ml of CH_3Li (1.7 M) in ether at 0 °C under N_2. After stirring for 1 h at room temperature, excess CH_3I (1 ml) was added at 0 °C and the solution stirred for 2 h at room temperature, to finally afford a colorless liquid, 0.606 g (66%).

Ethane	m/e 36	35	34	33	32	31	30	29	28	27	26
C_2D_6	25.1	2.8	18.3	3.2	100	6.8	23.1	1.3	16.3	0.8	1.3
CH_3CD_3	0	0	0	31.0	16.3	22.9	100	28.1	18.4	13.5	4.3
C_2H_6	0	0	0	0	0	0	29.0	23.4	100	30.2	19.0

***cis*-Et(CH$_3$)$_2$AuPMe$_3$.** $(CH_3)_3AuPMe_3$ (60 mg) in methylene chloride and 485 mg of iodine afforded *cis*-$(CH_3)_2AuI(PMe_3)$ (822 mg, 100%, mp 79–80 °C). *cis*-$(CH_3)_2AuI(PMe_3)$ (480 mg) was treated with EtMgBr (from 200 mg of Mg and 1 ml of EtBr in Et_2O) at 0 °C under N_2. A yield of 300 mg (80%) of a colorless liquid was obtained. The proton NMR spectral data of the alkylgold complexes used in this study are collected in Table VIII.

General. All solvents were purified by standard procedures, stored under nitrogen and distilled in vacuo before use. Methyllithium (Foote Mineral Co., halide-free) was used without further purification. The concentration of methyllithium was determined by quantitative gas chromatography of methane after hydrolysis. Alkyl halides were commercial samples and were redistilled before use. The NMR spectra were obtained on either a Varian EM360 or a XL-100 FT spectrometer. Mass spectra were measured on a AEI MS-9 spectrometer. Gases were analyzed by gas chromatography on 20 ft of dibutyl tetrachlorophthalate on Chromosorb-P and 2 ft of Porapak-Q at room temperature.

Kinetics of Cis–Trans Isomerization of *cis*-Et(CH$_3$)$_2$AuPPh$_3$. *cis*-$Et(CH_3)_2AuPPh_3$ and the requisite amount of PPh_3 were placed in an NMR tube sealed to a ⅋ joint. After evacuation, benzene was transferred by bulb to bulb distillation. The sealed tube was placed in a thermostated oil bath (70.0 ± 1.0 °C) and removed for NMR analysis. The ratio of cis and trans isomers was determined by measuring the peak height of the cis methyl resonance relative to PPh_3. In order to obtain more accurate ratios of the two isomers, calibration curves were prepared from known amounts of cis and trans isomers. The experimental error using this method was ±5%. In the absence of added PPh_3, gold deposited as a mirror, and the rate of isomerization was not determined quantitatively.

Kinetics of the Thermal Decomposition of *cis*-Et(CH$_3$)$_2$AuPPh$_3$. *cis*-$Et(CH_3)_2AuPPh_3$ was placed in the round-bottom flask equipped with a gas-tight rubber serum cap. Benzene was transferred by means of a hypodermic syringe and the flask evacuated. Isobutane was introduced and the flask placed in a thermostated oil bath at 70.0 ± 1.0 °C. Gas samples (less than 0.5% of the total volume) were removed periodically from the magnetically stirred flask, and analyzed by gas chromatography after calibration.

Thermal Decomposition of Deuterated Trimethylgold Complexes. In a typical procedure, 25.0 mg of *cis*-$CD_3(CH_3)_2AuPPh_3$ was placed in the round-bottom flask and 20.0 ml of decalin transferred. The system was evacuated completely and placed in a thermostated oil bath at 80.0 °C for 5 min. No gold metal deposited during this period. The gas was analyzed by connecting the flask directly to the mass spectrometer. The same results were obtained if the gas was first separated from the solvent manometrically and then analyzed.

Mass Spectral Analysis of Deuterated Ethanes. Ethane was collected by passing it through a dry ice–acetone trap in order to avoid contamination from the solvent, or analyzed directly by connecting the reaction mixture to the spectrometer. In the latter case, the solvent was analyzed separately. To obtain accurate cracking patterns for each component, authentic samples of C_2D_6, CH_3CD_3, and C_2H_6 were prepared. C_2D_6 was prepared by the decomposition of $(CD_3)_3AuPPh_3$ in decalin. CH_3CD_3 was obtained as follows: Deuterated ethanol (CD_3CH_2OH) was converted to ethyl bromide (CD_3CH_2Br) with 48% HBr solution and concentrated sulfuric acid in 80% yield bp 37–38 °C.[34] The deuterated ethyl bromide was found to be 98% isotopically pure (mass spectrum). After drying with CaH_2 overnight, the Grignard reagent (CD_3CH_2MgBr) was prepared from 100 μl of CD_3CH_2Br and 300 mg of Mg in diethyl ether (15 ml) under Ar. The Grignard solution was evacuated completely and 100 μl of distilled water was introduced by bulb to bulb distillation. The CH_3CD_3 was collected via several dry ice–acetone traps. C_2H_6 was a commercial sample. In order to check the sensitivity of the parent peak, a 1:1 mixture of CH_3CD_3 and C_3H_6 was prepared volummetrically with a mercury manometer. The mass spectral cracking patterns of normal and deuterated ethanes are tabulated at the top of this page. The peaks at 36, 33, and 30 were used for determining the composition of deuterated ethanes. The results were reproducible to within ±5%. The sample of CH_3CD_3 was employed as a daily check for sensitivity and reproducibility.

Table IX. Extended Hückel Parameters

Orbital	H_{ii}	Exponents[a] ξ_1	ξ_2
Au 5d	−15.07	6.163 (0.6851)	2.794 (0.5696)
6s	−10.92	2.602	
6p	−5.55	2.584	
C 2s	−21.40	1.625	
2p	−11.40	1.625	
H 1s	−13.60	1.300	

[a] Each Slater exponent is followed in parentheses by the coefficient in the double zeta expansion.

Reaction of Dimethylcuprate with Alkyl Halide. Dimethylcuprate was prepared in situ by mixing 190 mg of CuI and 2 mmol of CH_3Li at −78 °C in 20 ml of Et_2O under Ar. The system was evacuated at −78 °C to eliminate adventitious methane or ethane. CD_3I (114 mg) was introduced by bulb to bulb distillation and the mixture was allowed to warm to 0 °C. The gas consisted of only ethane. It was collected in a liquid N_2 trap after passing it through a dry ice–acetone trap.

The mixed dimethylcuprate $(CH_3)(CD_3)CuLi$ was prepared as follows. CuI (542 mg) was mixed with 3 mmol of CD_3Li in dry Et_2O at −78 °C under Ar. To the yellow heterogeneous mixture, 4 mmol of CH_3Li was added to afford a clear slightly yellow solution. Aliquots (5.0 ml) of this solution were used for the reaction with methyliodide, methyltrifluoromethanesulfonate, O_2, and acetic acid. The isotopic composition of the mixed ate complex was determined by acetolysis, which gave 66% CH_4 and 34% of CD_3H (mass spectral analysis).

Reaction of Dimethylaurate with CD$_3$I. Ligand-free dimethylaurate was prepared by mixing AuCl (230 mg) and CH_3Li (2 mmol) in dry Et_2O under Ar at −78 °C. A black insoluble precipitate was observed. The colorless supernatant solution was separated and treated with 114 mg of CD_3I in vacuo. The NMR spectrum of the colorless solution indicated the existence of free methyllithium (δ −1.84 ppm) together with dimethylaurate (δ 0.2 ppm). (The ratio was not determined.) Oxidation of this solution with concentrated H_2SO_4 afforded Au metal, and on standing for a day additional gold metal was produced. Since the extreme instability of this system prevented its thorough characterization, the results can only be accepted with reservations.

Molecular Orbital Calculations. The calculations on $(CH_3)_3Au$ were carried out by the extended Hückel method.[35] The parameters used are listed in Table IX. The gold d functions were taken as double zeta functions.[36] An Au–C distance of 2.10 Å, C–H of 1.10, and idealized tetrahedral angles in the methyl groups were used for the computations.

Acknowledgment. We wish to thank the National Science Foundation under Grant 28137 to Cornell University and Grant 742101 to Indiana University, and the Material Sciences Center at Cornell University for financial support, Dr. R. A. Budnik for the ^{31}P NMR spectra, Mr. R. J. Weber for the mass spectra, and Dr. J. Y. Chen for helpful suggestions.

References and Notes

(1) (a) Indiana University, (b) Cornell University.
(2) A. Tamaki, S. A. Magennis, and J. K. Kochi, *J. Am. Chem. Soc.*, **96**, 6140 (1974).
(3) (a) G. H. Posner, *Org. React.*, **22**, 253 (1975); (b) M. F. Semmelhack, *Ibid.*, **19**, 155 (1972), and R. Baker, *Chem. Rev.*, **73**, 487 (1973); (c) J. Kochi, *Acc. Chem. Res.*, 7, 351 (1974), and references therein; (d) D. Morrell and J. K. Kochi, *J. Am. Chem. Soc.*, **97**, 7262 (1975).
(4) (a) S. Stanley, W. Krauhs, G. C. Stocco, and R. S. Tobias, *Inorg. Chem.*,

10, 1365 (1971); (b) B. Armer and H. Schmidbaur, *Angew. Chem., Int. Ed. Engl.*, **9,** 101 (1970); (c) H. Schmidbaur and A. Shiotani, *Chem. Ber.*, **104,** 2821 (1971); (d) A. Tamaki and J. K. Kochi, *J. Organomet. Chem.*, **51,** C39 (1973).

(5) H. Gilman and L. A. Woods, *J. Am. Chem. Soc.*, **70,** 550 (1948); L. G. Vaughan and W. A. Sheppard, *J. Organomet. Chem.*, **22,** 739 (1970).

(6) A. Tamaki and J. K. Kochi, *J. Chem. Soc. A*, 2620 (1973); *J. Organomet. Chem.*, **51,** C39 (1973); G. E. Coates and C. Parkin, *J. Chem. Soc.*, 421 (1963).

(7) T. Yamamoto, A. Yamamoto, and S. Ikeda, *J. Am. Chem. Soc.*, **93,** 3350, 3360 (1971).

(8) (a) First proposed by A. Shiotani, H. F. Klein, and H. Schmidbaur, *J. Am. Chem. Soc.*, **93,** 1555 (1971); *Chem. Ber.*, **104,** 2831 (1971); (b) Cf. F. Basolo and R. G. Pearson, "Mechanism of Inorganic Reactions", 2d ed, Wiley, New York, N.Y., 1957, p 375.

(9) (a) The rate of reassociation in eq 20 is highly dependent on the structure of the phosphine ligand. Thus, PMe_3 is at least 10^3 times more effective than PPh_3 in retarding the isomerization of *cis*-$EtMe_2AuPMe_3$ (see Table V). (b) Note that ^{31}P NMR studies show that the retardation cannot be due to the formation of a five-coordinate species. (c) The equilibrium for ligand exchange in eq 18 is strongly displaced to the right.

(10) In addition to the unimolecular reductive eliminations in eq 23, k'_2 also includes (in decalin and benzene solutions) the contribution from the intermolecular pathways in eq 10.

(11) In order to apply the steady-state approximation, the fast (associative) equilibrium,

$$R(CH_3)_2AuS + PPh_3 \rightleftharpoons R(CH_3)_2PPh_3 + S$$

must also be included.

(12) For a description of the orbitals of CH_3 see W. L. Jorgensen and L. Salem, "The Organic Chemist's Book of Orbitals", Academic Press, New York, N.Y., 1973, pp 8 and 67.

(13) For previous theoretical discussions of T geometries for low spin three-coordinate d^8 complexes see (a) J. K. Burdett, *J. Chem. Soc., Faraday Trans.*, **70,** 1599 (1974); *Inorg. Chem.*, **14,** 375 (1975); (b) M Elian and R. Hoffmann, *ibid.*, **14,** 1058 (1975).

(14) Throughout this paper the simplified notation z^2, $x^2 - y^2$, xy, xz, and yz for the gold 5d orbitals and x, y, z for the 6p orbitals will be used.

(15) For a detailed account of the polarization phenomenon see L. Libit and R. Hoffmann, *J. Am. Chem. Soc.*, **96,** 1370 (1974). A specific application to an inorganic problem may be found in ref 13b.

(16) G. Herzberg, "Molecular Spectra and Molecular Structure", Vol. III, Van Nostrand Reinhold, Co., New York, N.Y., 1966, pp 45–51.

(17) W.-D. Stohrer and R. Hoffmann, *J. Am. Chem. Soc.*, **94,** 1661 (1972).

(18) J. M. Howell, unpublished.

(19) The LiH_3 system has also been studied by J. B. Collins, P. v. R. Schleyer, J. S. Binkley, J. A. Pople, and L. Radom, *J. Am. Chem. Soc.*, **98,** 3436 (1976).

(20) B. M. Gimarc, *J. Am. Chem. Soc.*, **93,** 593 (1971).

(21) The isoelectronic BeH_3^+ system has been studied theoretically by M. Jungen and R. Ahlrichs, *Mol. Phys.*, **28,** 367 (1974). See also J. Easterfield and J. W. Linnett, *Nature (London)*, **226,** 143 (1970). In this case the Y geometry is the minimum and a deformed T a transition state for interconversion of Y forms.

(22) R. E. Stanton and J. W. McIver, Jr., *J. Am. Chem. Soc.*, **97,** 3632 (1975).

(23) The choice of starting in the C_{3b} geometry rather than an alternative C_{3v}, motivated by the plan to attain a staggered rather than eclipsed ethane, has led us into a Y geometry whose only symmetry element is a nonessential mirror plane. The symmetry element decisive in making this an allowed or forbidden reactions is not a real one, but the one indicated in IX.

(24) For the ethane orbitals see ref 12.

(25) R. G. Pearson, *Acc. Chem. Res.*, **4,** 152 (1971); *Pure Appl. Chem.*, **27,** 145 (1971); *Fortschr. Chem. Forsch.*, **41,** 75 (1973).

(26) M. P. Brown, R. J. Puddephatt, and C. E. E. Upton, *J. Chem. Soc., Dalton Trans.*, 2457 (1974).

(27) (a) J. A. J. Jarvis, A. Johnson, and R. J. Puddephatt, *J. Chem. Soc., Chem. Commun.*, 373 (1973); (b) V. G. Andrianov, Yu. T. Struchkov, and E. R. Rossinskaya, *ibid.*, 338 (1973); *Zh. Strukt. Khim.*, **15,** 74 (1974); (c) P. W. R. Corfield and H. M. M. Shearer, *Acta Crystallogr.*, **23,** 156 (1967); (d) R. W. Baker and P. Pauling, *Chem. Commun.*, 745 (1969); (e) C. J. Gilmore and P. Woodward, *ibid.*, 1233 (1971); (f) M. A. Bennett, K. Hoskins, W. R. Kneen, R. S. Nyholm, P. B. Hitchcock, R. Mason, G. Robertson, and A. D. C. Towl, *J. Am. Chem. Soc.*, **93,** 4591 (1971); (g) W. P. Fehlhammer and L. F. Dahl, *ibid.*, **94,** 3370 (1972); (h) G. E. Glass, J. H. Konnert, M. G. Miles, D. Britton, and R. S. Tobias, *ibid.*, **90,** 1131 (1968); (i) P. C. Bertinotti and A. Bertinotti, *Acta Crystallogr., Ser. B*, **28,** 2635 (1972); (j) M. McPartlin and A. J. Markwell, *J. Organomet. Chem.*, **57,** C25 (1973); (k) L. Manojlovic-Muir, *ibid.*, **73,** C45 (1974).

(28) (a) C. R. Johnson and G. A. Dutra, *J. Am. Chem. Soc.*, **95,** 7783 (1973). See also G. M. Whitesides, W. F. Fisher, Jr., J. San Filippo, Jr., R. W. Bashe and H. O. House, *ibid.*, **91,** 4871 (1969); (b) H. O. House, *Acc. Chem. Res.*, **9,** 59 (1976), and references therein.

(29) This system is uncharacterized as yet. See A. Tamaki and J. K. Kochi, *J. Organomet. Chem.*, **51,** C39 (1973); G. W. Rice and R. S. Tobias, *Inorg. Chem.*, **14,** 2402 (1975).

(30) (a) W. H. Mandeville and G. M. Whitesides, *J. Org. Chem.*, **39,** 400 (1974).

(31) These results, of course, do not favor either mechanism.

(32) (a) Reductive eliminations from binuclear intermediates have been previously proposed, G. E. Coates and C. Parkin, *J. Chem. Soc.*, 421 (1963); A. Tamaki and J. K. Kochi, *J. Organomet. Chem.*, **61,** 441 (1973); F. Ungvary and L. Marko, *ibid.*, **20,** 205 (1969); J. Evans and J. R. Norton, *J. Am. Chem. Soc.*, **96,** 7577 (1974). (b) The absence of intermolecular scrambling between $(CH_3)_3AuL$ and $(CD_3)_3AuL$ previously reported[2] was carried out in very dilute solutions and is not generally applicable. Since there is no scrambling in the reactants, reductive elimination must proceed from the binuclear intermediate faster than redissociation. (c) For binuclear Au intermediates in Me exchange see G. W. Rice and R. S. Tobias, *J. Organomet. Chem.*, **86,** C37 (1975); J. P. Visser, W. W. Jager, and C. Masters, *Rec. Trav. Chim. Pay-Bas*, **94,** 70 (1975).

(33) The preferential elimination of propane from $Et(CH_3)_2Au$ may either be due to a favored deformation of the T configuration or different rates of reductive elimination of ethyl and methyl groups. In either case, these studies show that $R(CH_3)_2AuL$ ($R \neq CH_3$) are not suitable models for stereochemical studies in which an ethyl or other primary alkyl groups are used as methyl labels. Although we now arrive at some of the same conclusions regarding R_3Au, this is not for the reason previously given.[2]

(34) A. Tsolis, P. P. Hunt, J. K. Kochi, and S. Seltzer, *J. Am. Chem. Soc.*, **98,** 992 (1976).

(35) R. Hoffmann, *J. Chem. Phys.*, **39,** 1397 (1963); R. Hoffmann and W. N. Lipscomb, *ibid.*, **36,** 2179 (1962); **37,** 2872 (1962).

(36) H. Basch and H. B. Gray, *Theor. Chim. Acta*, **4,** 367 (1966).